Enhancing drought resilience and energy security through complementing hydro by offshore wind power—The case of Brazil

Borba, Paula Conde Santos; Sousa, Wilson C.; Shadman, Milad; Pfenninger, Stefan

DOI
10.1016/j.enconman.2022.116616

Publication date
2023

Document Version
Final published version

Published in
Energy Conversion and Management

Energy Conversion and Management 277 (2023) 116616

Contents lists available at ScienceDirect

Energy Conversion and Management

journal homepage: www.elsevier.com/locate/enconman

Enhancing drought resilience and energy security through complementing hydro by offshore wind power—The case of Brazil

Paula Conde Santos Borba [a,b,*], Wilson C. Sousa Júnior [a], Milad Shadman [c], Stefan Pfenninger [b]

[a] Department of Civil Engineering – Aeronautics Institute of Technology (ITA), Praça Marechal Eduardo Gomes 50, São José dos Campos, 12228-900, São Paulo, Brazil

[b] Faculty of Technology, Policy and Management - Delft University of Technology, Jaffalaan 5, Delft, 2628BX, The Netherlands

[c] Offshore Renewable Energy Group (GERO), Ocean Engineering Department, COPPE, Universidade Federal do Rio de Janeiro, R.Moniz Aragão 360, Rio de Janeiro, 21941-594, Brazil

ARTICLE INFO

Keywords:
Offshore wind energy
Hydropower
Renewables complementarity
Energy modeling
Drought management
Bias correction

ABSTRACT

During atypical droughts, power systems with a heavy reliance on hydropower risk increased greenhouse gas emissions if they are balanced with fossil-fired generation. This work investigates the role of offshore wind energy in reducing the vulnerability of power systems dependent on such hydrological patterns, thereby eliminating this emission increase, using Brazil as a case study. Offshore wind potential and its complementarity with hydro resources are addressed by considering bias-corrected reanalysis data. Then, a cost-minimizing model is built to analyze the effect of integrating wind farms (considering bottom-fixed and floating structures and distance to shore) into the existing power system in Brazil. Applying a lower, median, and upper bias correction factor, potentials are reduced by 8%–44% compared to uncorrected data. Irrespective of systematic bias, the findings indicate a high complementarity between Northeastern wind regimes and most hydropower basins. The share of offshore wind energy grows in scenarios with reduced costs, but wind farms are part of the optimal system even with the current costs. With increasing wind power capacity, dynamic dispatch changes, and natural gas no longer plays a role in the dry season as it currently does, but only in the rainy season on a significantly reduced scale. Existing reservoirs support the integration of offshore wind farms into highly renewable scenarios, but they are insufficient in a complete fossil fuel phaseout, where other electricity storage must be deployed to help balance the system. Yet, power systems in the scenarios with large wind capacity have less stored hydropower in the dry season than in the current system, while they store more in the rainy season, implying a reduced risk of empty reservoirs. The Brazilian power system with offshore wind farms can eliminate 54.4 Mton $CO_{2eq}/year$ (97% of current power sector emissions) without additional electricity storage.

1. Introduction

Hydropower represents 62% of global renewable electricity generation [1] and supports the economic growth of many developing countries due to its low cost and locally large power production capacity [2]. However, atypical droughts have increased in recent years [3] and will likely exceed their usual magnitude in some regions of the globe due to climate change [4]. In terms of energy, lack of water is a concern for countries dependent on hydropower. That is the case for Brazil, which has been facing anomalous hydrological cycles [5,6], threatening its large hydropower fleet, which represents 56% of installed electricity generation capacity (both run-of-river and reservoirs) [7].

The problem goes beyond the lack of hydro resources. First, to compensate for the low water availability, grid operation currently relies on firm power, which is provided mainly by fossil fuels. Although the hydro-thermal dispatch model is well-known and assured power during dry seasons, the use of fossil fuel-fired backup generation, particularly based on natural gas, became more frequent due to an increase in the recurrence of prolonged droughts [8], intensifying the Greenhouse Gas (GHG) emissions from the power sector. Second, to bolster Brazil's energy security, thermal power stations based on domestically-produced natural gas may receive more investment in the near future [9], despite the need to phase out fossil fuels globally.

* Corresponding author at: Department of Civil Engineering – Aeronautics Institute of Technology (ITA), Praça Marechal Eduardo Gomes 50, São José dos Campos, 12228-900, São Paulo, Brazil.

E-mail address: paula.borba@ga.ita.br (P.C.S. Borba).

https://doi.org/10.1016/j.enconman.2022.116616
Received 1 August 2022; Received in revised form 16 December 2022; Accepted 19 December 2022
Available online 29 December 2022

Offshore wind energy has become a large-scale alternative, particularly in Europe and China, to achieve the goal of reducing fossil fuel reliance [10]. The wind power industry has matured and the future cost of offshore wind farms is promising [11]. Also, wind farms at sea reduce the land-use conflicts caused by other onshore technologies [12], especially in countries where land availability or land conflicts might be an issue.

In Brazil, offshore wind energy is not yet exploited, although it has one of the largest potential resources in the world, much of which is close (10–50 km) to shore [13]. The Northeast has most of the areas suitable for offshore wind development [14], but the Southern and the Southeastern regions also have significant potentials [15]. Although wind potentials are high, integrating large amounts of additional variable renewable generation requires the adaptation of a power system largely dependent on already-fluctuating hydro resources.

Silva et al. [16] suggest a synergy between offshore wind energy and hydro resources in Brazil, particularly during the dry season. The authors applied Pearson's correlation to assess their complementarity. Similarly, adopting the Spearman correlation method, Gonzalez-Salazar et al. [17] showed that onshore wind–solar systems have potential to compensate hydropower fluctuations in Latin America. However, their work leaves out the integration of wind power into energy systems. Brazilian offshore wind potential and cost-related studies, such as the Roadmap made by the government [15,18], use reanalysis data that contain systematic errors (biases). Although global reanalysis data makes it possible to estimate renewable resources remotely by incorporating atmospheric observations with forecast models to cover the entire world, the resulting wind power estimates have been shown to suffer from substantial bias [19], including in Brazil [20]. Tavarez et al. [21] validate reanalysis data with meteorological data, but their study focuses only on the Southeastern coast of Brazil.

To fill these gaps, this work investigates the potential contribution of offshore wind energy to enhance energy security and reduce the use of fossil fuels in a power system that is already fluctuating. For that, a novel model of the Brazilian power system was built, leading to three additional findings: optimal offshore wind farm locations considering spatial constraints; dynamics of storage technology operation throughout the year, and alternatives to reduce power sector GHG emissions. Besides modeling, two further assessment was carried out: estimated Brazil's offshore wind potential with bias-corrected reanalysis data and the dynamics of combining offshore wind with hydropower by analyzing their complementarity. That evaluation identifies relevant existing hydro systems and potential offshore locations in the context of wind energy expansion. Finally, this work provides a guide for developing offshore wind energy in highly renewable power systems. This supports Brazilian policymakers in finding pathways to sustainable and low-emission energy systems.

The model has been deposited to Zenodo https://doi.org/10.5281/zenodo.6767868. Results and additional data are available on: https://doi.org/10.5281/zenodo.6855581.

2. Methods

Fig. 1 provides an overview of the main analysis steps. First, the geospatial analysis consists in defining the geographical nodes for wind power deployment based on a Geographical Information System (GIS) and the assessment of available areas. Second, the pre-processing phase includes the simulation of the wind power and its bias correction, which leads to a validated potential of Brazilian offshore wind energy. The third step involves the analysis of the complementarity between wind and hydro resources. Finally, the power system model is built with high spatial resolution, combining wind, hydro, and electricity demand time series.

2.1. GIS analysis

The 350 offshore spatial nodes have a resolution of 0.5° × 0.5° (Fig. 2). The available area is limited by a maximum water depth of 1000 meters and a distance to shore between 8 and 200 km. These constraints are based on Vinhoza et al. [14]. Regions with a concentration of migratory birds and protected areas were excluded [22]. The spatial data for water depth used in this work are from CPRM [23], for bird and protected areas, from the Ministry of Environment [24].

The maximal capacity of a particular zone depends on the available area to place wind turbines. Every node has a square buffer (0.5°× 0.5°), and the area within that buffer is grouped by six intervals of water depth: 0–20 m, 20–50 m, 50–75 m, 75–100 m, 100–200 m, and deeper than 1000 m.

2.2. Offshore wind power: simulation, bias correction, and potential

The wind power for the nodes described in Section 2.1 is simulated at hourly resolution considering two decades of data (2000–2019). The wind power time series are obtained from Renewables.ninja, a platform based on reanalysis data from NASA's MERRA-2 [25]. Renewables.ninja combines wind speeds at different heights provided by MERRA-2 and interpolates them according to the geographic coordinates and hub height, both given by the user, and then converts the speeds to power outputs using power curves from the turbine manufacturers [19]. The assumptions to run the wind power simulation are the turbine V164 8MW from Vestas and a hub height of 100 m. The capacity factors are given by dividing the output power production by the rated turbine power.

In the absence of offshore wind farms, the bias is corrected by using Renewables.ninja to simulate capacity factors of existing onshore wind farms near the sea and compare them to actual capacity factors. To reproduce precisely the wind performance, the simulation relies on the power production of 206 wind farms using their technical specifications given by ABBEólica. In case of missing values, turbine models with the same rotor diameter or capacity in the technical data are adopted.

The Operator of The National Power System (ONS, in Portuguese) [8] provides data for monthly wind power generation, making it possible to match them with the simulated reanalysis data. The following data were not part of the analysis to avoid having inaccuracy or low representation of time series: data with less than three years of recorded data, and farms with no statistical significance in the linear correlation between observed and simulated capacity factors. The low correlation might indicate flaws during data record and collection.

The biases are grouped by state, and their values from the 25th, 50th and 75th percentile are used to correct the reanalysis data. Staffell and Pfenninger [19] applied an additional coefficient for offshore wind calibration in Europe based on actual references to reproduce the absence of obstacles at sea that could obstruct airflow. Since there are no offshore wind references for Brazil and only farms near the coast were selected, the additional coefficient is not included.

The offshore wind potential assessment (later used to build the model) includes nodes with a minimum annual average capacity factor of 45% (or wind speed higher than 8.5 m/s). That assumption considers that there are no existing onshore wind farms in regions with low wind potential, and thus, there is no reference for the power output and the bias correction. There are, however, existing onshore farms near the regions where offshore power potential is also high. Further, computational limitations in running large power system models based on linear optimization (see below) make it necessary to make a preselection of nodes. For the complementarity analysis (Section 2.4), all offshore nodes are considered since that does not depend on the capacity factor magnitudes, i.e., the bias correction does not affect the results of hydro-wind synergy.

The potential of electricity generation is an output from the available area multiplied by a capacity density of 5.2 MW/km^2, estimated

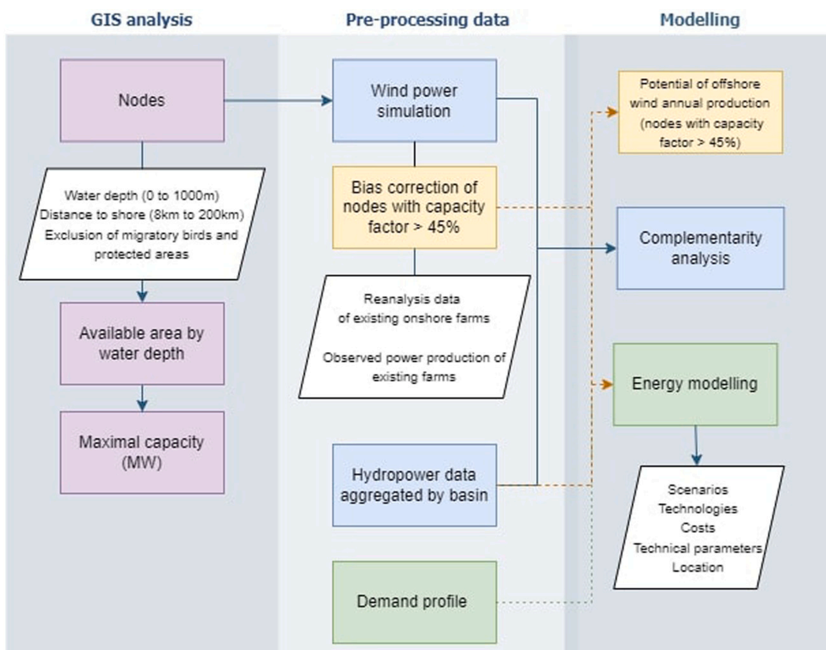

Fig. 1. Flowchart of methods used.

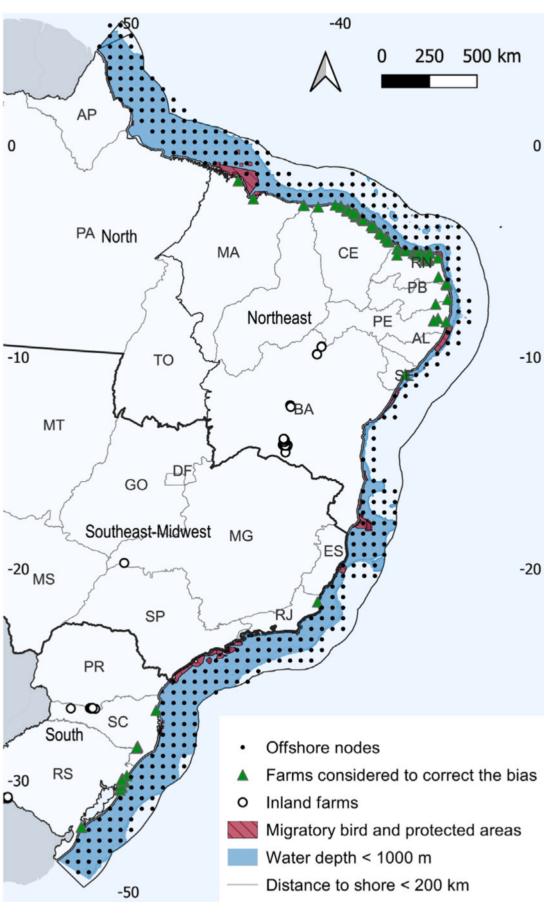

Fig. 2. Offshore nodes and spatial constraints.

according to turbine distances of $10D$ and $5D$ in an x-y-axis, where D is the rotor diameter [26]. The electricity production potential (E) follows Eq. (1):

$$E_i = d * A_i * CF_{it} \tag{1}$$

in which i represents the location, d is the capacity density in MW/km^2, A is the available area in km^2, and CF is hourly capacity factor (t).

Seasonality in the built model has two seasons: dry and rainy. The dry season occurs during the winter in almost every region of Brazil (except the far Northern part) [16] and lasts from 21st June to 23rd September, while the rainy season covers the remainder of the year [27].

2.3. Hydropower

Available hydropower (also called Affluent Natural Energy) depends on the hydrological balance and the productivity of a hydropower plant. The cascades of hydropower plants combined with the linkages among water bodies allow exchanging flows, increasing the control over hydropower dispatch and storage and making precise modeling of hydropower assets challenging. Here, the data used are from ONS, obtainable for all run-of-rivers and reservoirs operated by ONS [8]. To capture the cascade effect and the interchangeability of the hydro resources, hydropower plants are in groups of basins (Fig. 3). Moreover, hydropower time series are split into run-of-river and reservoir based on the installed capacity of both technologies.

This work considers 20 years of hydro data (2000–2019) since inter-annual variation might be significant. However, the hydro time series obtained from ONS rely on the installed capacity when data is collected, therefore also capturing the effect of changes to the hydropower fleet through time. To obtain an estimate of how the current fleet would have performed through these 20 years, the observed data were multiplied by the ratio of current installed capacity to the capacity at each past moment. Moreover, data with negative or missing values are corrected by considering the last non-negative number at the nearest date.

Fig. 3. Hydropower plants aggregated by basin.

In a reservoir, the remaining Affluent Natural Energy, accumulated over a certain period, works as potential electricity storage. The maximal storage in a basin, given in GWh, results from the sum of maximal storage from individual reservoirs. The minimum operation level to maintain the river's ecosystem and its navigability limit the usage of stored hydro resources. Thus, the maximal storage has a limit following the average security levels adopted by ONS [28].

2.4. Complementarity analysis

The correlation coefficient is the most popular measure of dependence between two randomly distributed variables [29]. Pearson's and Kendall's correlations are basic methods to assess the complementarity between renewable resources. However, using Pearson's correlation requires the presence of a linear relationship, normal distribution, and homoscedasticity between the variables, while Kendall's correlation does not have these assumptions [30]. Because wind power and hydropower hardly meet these assumptions, Kendall's correlation coefficient was used to evaluate their complementarity. Kendall's correlation coefficient (τ) is given by:

$$\tau = P\{(w_i - w_j)(h_i - h_j)\} > 0 - P\{(w_i - w_j)(h_i - h_j)\} < 0 \tag{2}$$

where P represents the probability of an event, and (w_i, h_i) and (w_j, h_j) are two independent pairs from the wind (w) and hydropower (h) time series. The first term on the right of Eq. (2) is called the concordance term, and the left, discordance. The signal of τ varies from −1 to 1 and represents the direction and the magnitude of the correlation. Coefficients near or equal to zero mean that there is no correlation. The more negative the coefficient is, the stronger the complementarity, while the more positive, the more synchronous the variables are.

2.5. Power system modeling

The model of the Brazilian power system is built using Calliope, an open-source energy modeling tool based on linear optimization [31] with the objective function of minimizing total system cost. Calliope is flexible and allows the user to create different scenarios given a set of constraints that the user also assigns. The outputs include the balance of the energy system, costs including Levelized Cost of Electricity (LCOE), and $CO_{2_{eq}}$ emissions. Moreover, Calliope is appropriate for highly renewable systems since the framework can incorporate resource fluctuations through time series and spatial nodes. For this study, a temporal resolution of 6 h is considered, which is sufficient to cover the desired scale of variability to depict in studying the combination of wind and hydropower resources.

2.5.1. Technologies, costs, technical assumptions, and locations

The model includes offshore wind farms, run-of-river, and reservoir-based hydropower plants, combined-cycle gas turbine (CCGT) power stations, grid-connected batteries, electrolyzers, and green hydrogen compression and storage (hydrogen is permitted to be produced only by offshore wind farms).

Wind farms are in groups according to their foundation type: monopile, jacket, or floating. Fixed bottom foundations include monopile and jacket and are limited by a maximal water depth of 100 m [32]. Floating structures are permitted up to a depth of 1000 m. In the model, floating technologies are only used between depths of 100 and 1000 m, although their installation is also possible in shallow waters. The distance to shore is represented by average value. Distances of 25 km represent nodes located between 0–50 km from shore, 75 km nodes between 50–100 km, 125 km between 100–150 km, and 175 km between 150–200 km.

Technology costs include capital expenditures (capex), operational expenditures (opex), fuel, and storage costs. For conventional and mature technologies, such as hydropower plants, CCGT, and coal+oil-based thermal power plants, the cost assumptions are given by EPE (Energy Research Office) [9]. The fuel price for natural gas represents the average value of the cost range, also reported by EPE. For electrolyzers and hydrogen storage, the reference for estimated costs are from [33], and for batteries, costs are from [34].

Finding actual and detailed costs of offshore wind farms is challenging because most project information is confidential. In this work, farm costs are based on equations compiled by Tavares et al. [21] and indicated in Table 1. The equations include costs of project development, turbines, substructures, electrical interconnection, export cables, installation, and operation.

In the model, the time series of variable resources include turbine efficiency. For other technologies, the conversion efficiency is available in Table 1. Data for technology life-cycle emissions of $CO_{2_{eq}}$ are based on the IPCC Fifth Assessment Report [35]. This work compares life-cycle emissions from natural gas and offshore wind farms. While hydropower plants can also exhibit substantial lifecycle emissions, it was assumed no change to the hydropower fleet and not accounted for total energy sector emissions, thus, can be excluded those emissions from the analysis.

Geographical nodes are inputs in Calliope. However, the more nodes, the higher the computational costs. To simplify the model, nodes with a capacity factor higher than 45% are added to the model. Thus, zones that would be unattractive to the cost-minimizing model are not considered, while keeping a high level of detail.

After calculating the maximal capacity described in Section 2.1, nodes with a capacity smaller than 300 MW are not part of the model since the costs of offshore infrastructure might would likely be too high to build relatively small farms. For hydro resources, the locations are the basins, which are described in Section 2.3.

Part of this analysis includes identifying optimal locations for offshore wind farms.

2.5.2. Demand

ONS provides 20 years of hourly demand profiles [36], which, for this work, past demand time series were updated using as a reference the demand peak in 2019. This year was selected because it is the most recent year before the COVID-19 pandemic, when electricity demand dropped due to confinement measures.

Table 1
Costs and technical parameters.

Technology	Capital (US$/MW)	Operation (US$/MW/yr)	Fuel (US$/MWh)	Storage costs (US$/MWh)	Efficiency (%)	Emission (ton $CO_{2_{eq}}$ /MWh)	Lifetime (yr)
Reservoir-based hydropower plant		12,820	–	–	–	–	30 –
Run-of-river	–	12,820	–	–	–	–	30 –
Combined Cycle Gas Turbine (CCGT)	1,077,000	43,590	43.46	–	0.58	0.490	20
Coal and oil-fired power station	2,250,000	89,740	96.33	–	0.40	0.820	25
OWF- Monopile 25 km to shore	3,605,226	61,616	–	–	–	0.010	20
OWF - Jacket 25 km to shore	4,085,245	61,616	–	–	–	0.010	20
OWF - Jacket 75 km to shore	6,521,195	71,768	–	–	–	0.010	20
OWF - Floating 25 km to shore	3,845,229	61,616	–	–	–	0.010	20
OWF - Floating 75 km to shore	6,281,178	71,768	–	–	–	0.010	20
OWF - Floating 125 km to shore	8,717,128	83,486	–	–	–	0.010	20
OWF - Floating 175 km to shore	11,153,078	96,770	–	–	–	0.010	20
4h Battery - Lithium-ion systems	1,318,000	33,000	–	259,000	0.85	–	15 –
Electrolyzers	600,000	12,000	–	–	0.70	–	30
Hydrogen - Compression and storage	257,600	2,576	–	6496	–	–	20

Table 2
Scenarios and layers.

Scenario group	Scenario name	Layer A: cost	Layer B: weather	Layer C: wind model bias
Baseline	Baseline	Status quo		
Offshore Wind Farms (OWF) - capex reduction	OWF_capex_10	capex reduced by 10%		
	OWF_capex_30	capex reduced by 30%		
	OWF_capex_50	capex reduced by 50%		
	OWF_capex_70	capex reduced by 70%	Hydropower, wind power and demand time series from 2000 to 2020	Lower, median and upper cases of bias correction factor
Natural gas prices	Gas_low	$24/MWh		
	Gas_high	$62/MWh		
Gas-high + capex reduction	Gas-high + OWF_capex_10			
	Gas-high + OWF_capex_30			
	Gas-high + OWF_capex_50			
	Gas-high + OWF_capex_70			
Fossil fuel phase-out	Fossil fuel phase-out	Status quo		

Since this study focuses on offshore wind, hydro, and fossil fuels, the electricity generation from all other resources was removed from electricity demand. The fluctuating nature of existing onshore wind and solar power influences the demand profile. Thus, the power of existing wind and solar farms was simulated with the same 20 years of reanalysis-based weather data and their bias correction. For small hydropower plants, nuclear and biomass-based power stations, the power generation in 2019 is assumed, which is an acceptable simplification given the small share of power generation from run-of-river plants with a capacity lower than 30 MW (3.5%), and the inflexible nature of nuclear and biomass-fired generators that use the waste from biofuel manufacturing processes.

2.5.3. Scenarios

Four main scenarios explore the system configuration's sensitivity to technology cost. Table 2 shows the scenarios and the three layers that define combinations of assumptions.

The baseline scenario represents the state-of-the-art, while scenarios with new technologies (offshore wind farms, battery, and hydrogen) explore the system's configuration when capex is reduced. In the "Natural gas prices" group of scenarios, low and high costs are based on the current range of costs published by EPE [9]. Next, the configuration "Gas-high" is combined with the reduction of OWF-capex. Scenarios include 20 years of historical weather conditions, minimizing the risk of results being influenced by reliance on a single and atypical weather year. Thus, for instance, the scenario group "OWF-capex reduction" has four options in Layer A, 20 options in Layer B, and three options in Layer C, which results in a total of 240 scenarios. The overall total number of scenarios is 720.

3. Results and discussion

This section presents the bias-corrected offshore wind potential, the complementarity analysis between wind and hydro resources, and results from the power system modeling, which includes optimal system designs, the role of storage technologies, and emissions reduction potential.

3.1. Offshore wind power: bias correction and annual potential

Simulated outcomes show a high potential over the Southeastern, Southern, and Northeastern coasts (Fig. 4). During the dry season, capacity factors increase, on average, by 13%, 15%, and 38% in the Southeast, South, and Northeast, respectively. In the North, capacity factors decrease 18% during dry periods. However, those results are based on reanalysis data without bias correction.

MERRA-2-based wind power simulation contains significant bias, which is in line with results from [37]. The biases differ significantly at a farm level, as indicated in Fig. 5. In most cases, MERRA-2 overpredicts the wind power but underpredicts in Rio de Janeiro (RJ), Pernambuco (PE), and some wind parks in Piauí(PI). Tavares et al. [21] also found lower potentials with MERRA-2 compared to ERA5 and CFSv2, and highlighted a better performance of ERA5 when validated with an anemometer in the Southeast.

Although MERRA-2 simulation has a clear bias, the monthly and inter-annual variability between observed and simulated power is similar (see Supplementary Material). Data from farms in Santa Catarina had no correlation between observed measurements and simulated data at a reliable statistical level. Data of wind farms in Maranhão (MA) have time series shorter than three years. Therefore, these states were not included in the analysis.

Assuming a single bias to correct the reanalysis data might lead to inaccurate conclusions since biases vary at the farm level. To avoid this, the first quartile, the median, and the third quartile of biases by state are used to obtain corrected reanalysis data of selected nodes.

Fig. 6 shows the nodes with a capacity factor higher than 45%, and Fig. 7 shows the annual production at different levels of water

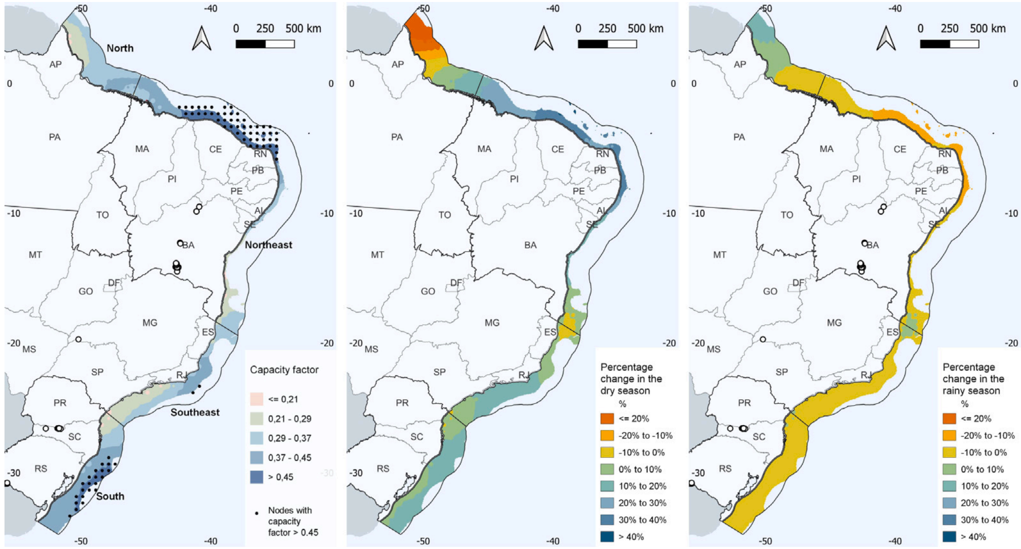

(a) Annual average of capacity factor (b) Percentage change in the dry season. (c) Percentage change in the rainy season.

Fig. 4. Simulated offshore wind capacity factors without bias correction.

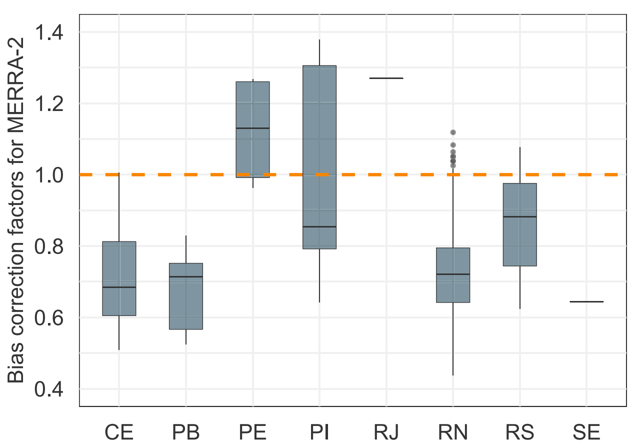

Fig. 5. Boxplots of wind power bias at farm level aggregated by state.

depth. Regardless of the bias case, the largest potential is over regions with deeper water (>200 m), followed by regions with shallow water (<50 m). The total wind power production potential is 2366 TWh/yr without bias correction. In the case of upper bias, the potential is reduced by 8%, while for median and lower bias cases, by 25% and 44%, respectively. Water depth between 100 and 200 m presented the lowest variation compared to simulated data without correction. The highest variation occurred for the interval between 0 to 20 m.

The uncorrected simulation differs from results reported by EPE [15]. For water depths of 20 m, both studies resulted in the same value (296 TWh). For water depths between 20 and 50 m, the results of this work are 92 TWh higher, while for 50 and 100 m, the potential is 165 TWh lower. Those differences occur because of two main reasons. First, EPE indicates the gross potential without excluding areas with environmental and social restrictions. Thus, area availability is different and impacts the total potential. Second, EPE adopted a capacity density of 3.18 MW/km^2 (on average), while this work considers 5.2 MW/km^2.

3.2. Complementarity analysis

The correlation coefficients diverge according to the temporal resolution adopted. For longer time scales, the long-term climate patterns prevail, while for short time scales, local terrain and real-time conditions affect the weather variables, decreasing the coefficient's magnitude [30]. Here, results from the monthly scale are presented, while results from the daily scale are available in the Supplementary Material. All coefficients were statistically significant at 1%. That indicates a risk level lower or equal to 1% in concluding that a correlation exists when there is no correlation or vice-versa.

On the monthly scale, Kendall's coefficients vary from 0 to 0.70, or from no synergy to the highest complementarity. Basins from the South presented a different pattern than other regions (Fig. 8). While their complementarity with Northern wind is higher than other basins, the Southern basins have lower or no synergy with wind regimes over most of the coast. In contrast, other basins (Figs. 9 and 10) show complementarity with wind regimes on the entire coast (apart from the North), although with different magnitudes.

Hydro resources in the Amazonas basin have a homogeneous negative correlation with wind resources (except in the North). However, its synergy is weaker compared to other basins. On the other hand, results show a better complementarity between basins from the Southeast and Northeast and wind regimes over most of the coast, particularly in the Northeast. Tocantins, Paranaíba, Parnaíba and Paraná have the highest complementarity with Northeastern wind.

In climate change scenarios, run-of-river plants are more vulnerable as they operate with lower flexibility and depend on the river flow [38]. Reservoirs may also suffer the impacts of droughts on reduced water levels, but their water storage enables supply compensation over the year. Of all basins, run-of-river plants have the highest share in the Amazonas basin, with a capacity of 22.7 GW. A decline in stream flow, particularly in the dry season, has been observed in the Southern Amazonas basin [39,40]. EPE [9] indicates 68 GW of inventoried and not yet developed hydro potential, primarily concentrated in Amazonas and Tocantins-Araguaia. However, the results imply that in a context of rapid expansion of wind technologies, new hydropower plants in these regions should be rethought, given that run-of-river plants in the Amazonas basin have weaker complementarity with offshore wind regimes and might be vulnerable to drought. In contrast, the power system might benefit from the high complementarity between wind power and existing run-of-river plants in the Southeast Midwestern, which has 20 GW of capacity.

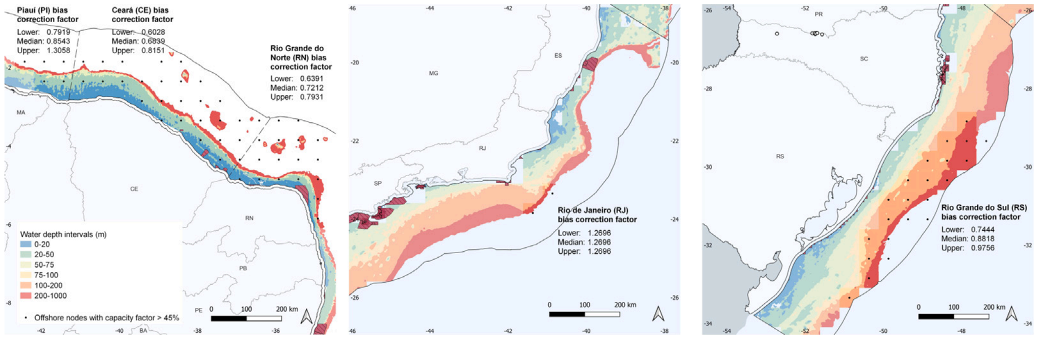

(a) Northeast. (b) Southeast (c) South.

Fig. 6. Nodes with capacity factor higher than 45%.

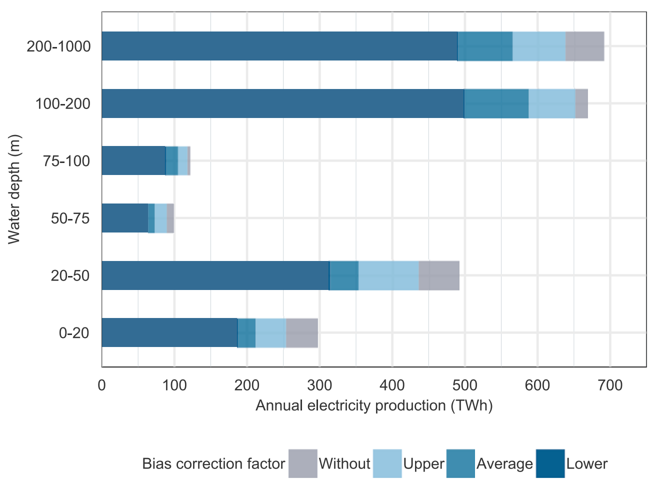

Fig. 7. Potential of annual wind power production.

3.3. Optimal systems

Model runs include three cases of wind power: lower, median, and upper values for the bias correction factor. The main difference between the three cases is in each scenario's wind capacity and power production, as indicated in Fig. 11. Results show a larger share of natural gas in the lower case, but it becomes smaller in scenarios with a more significant reduction of wind farm capex due to the increase of wind capacity. For all cases, wind power production is increased with the reduction of capex, while natural gas-fired is decreased. However, the intersection between the wind and gas lines (or when wind production overcomes gas power) happens with a small capex reduction in the upper case, followed by the median case. In the scenario gas+high and the capex reduced by 50% and 70%, the wind bias cases do not affect the power generation.

To avoid extensive results, the results of the median bias case are discussed. Results from lower and upper cases of bias correction factor are available in the supplementary material.

In a cost-minimal system where fossil fuel is allowed, electricity demand is covered by wind, hydro and CCGT technologies, without the need for either batteries or hydrogen for electricity storage. In "Fossil fuel phase-out", hydrogen production and conversion to power are part of the solution since they are needed for storage. The optimal system configuration changes over the different weather years due to the annual variability of wind and hydro resources. Fig. 12 shows the capacity, on average, over the weather years, as well as in the best and worst single years in terms of total hydropower availability.

Scenarios Gas-high+OWF-capex 70% and 50%, and OWF-capex 70% had similar optimal systems and the largest share of wind capacity among the scenarios. The total capacity increases by around 20 GW compared to the baseline in the median case. Offshore wind farms with capex reduced by 10% are not cost-competitive, but they become viable when combined with the high price of natural gas. When wind farm costs are reduced by 70%, natural gas prices do not have any effect on the optimal system. These results suggest that even in absence of further climate policy interventions, and assuming that the relative cost difference between wind and gas changes in favor of wind, wind power likely becomes a more economically attractive option for complementing existing hydropower generation, compared to gas.

The wind capacity increases when hydro resources are scarcer, but only for scenarios with a larger wind share. In scenarios Gas-high OWF-capex 70% and 50%, and OWF-capex 70%, wind capacity increases nearly by 86% in the worst hydro year, compared to the best year. Meanwhile, in scenarios that include wind capacity but natural gas is still relevant, the model revealed a reduction in wind capacity in the worst year and an increase in gas share.

Without wind technologies, natural gas is essential during the dry season, as observed in Fig. 13. That configuration changes in scenarios Gas-high+OWF-capex 70% and 50%, and OWF-capex 70%, where wind capacity is more significant. Thus, although natural gas is part of all optimal systems considered in this work, its seasonal function changes since its relevance is decreased in the dry season but remains necessary to meet demand in the rainy season.

The 20 different weather year scenarios depict inter-annual variability. Fig. 14 shows the weather sensitivity of scenario "Gas-high + OWF-capex-70%". Results suggest an increase in wind capacity when the weather years are ordered from the worst to the best hydro year in terms of total available hydropower. Although 2001 was the worst year in general, 2003 had the lowest water availability during the dry season, explaining the larger wind capacity. Scenarios with a lower wind share are less sensitive to hydropower years.

3.4. Offshore wind farms: structures, costs, and locations

Fig. 15 shows the capacity of wind technologies by scenarios. Monopile-based wind turbines account for 100% of all wind capacity in scenarios Gas-high and capex-30%, and 71% in Gas-high+capex 10%, while in other scenarios, they are on average around 48%. Jacket foundation shares vary from 20% to 37%. With the cost reduction in scenarios Gas-high+OWF-capex 70% and OWF-capex 70% floating structures are around 34% among wind technologies, and 25% for Gas-high+OWF-capex 50%.

Usually, the higher the distance from shore, the higher the wind speeds. In scenarios where capex is reduced by 70%, wind locations farther than 50 km are used more than in other scenarios. Monopile-based farms have a lower capacity in those scenarios compared to

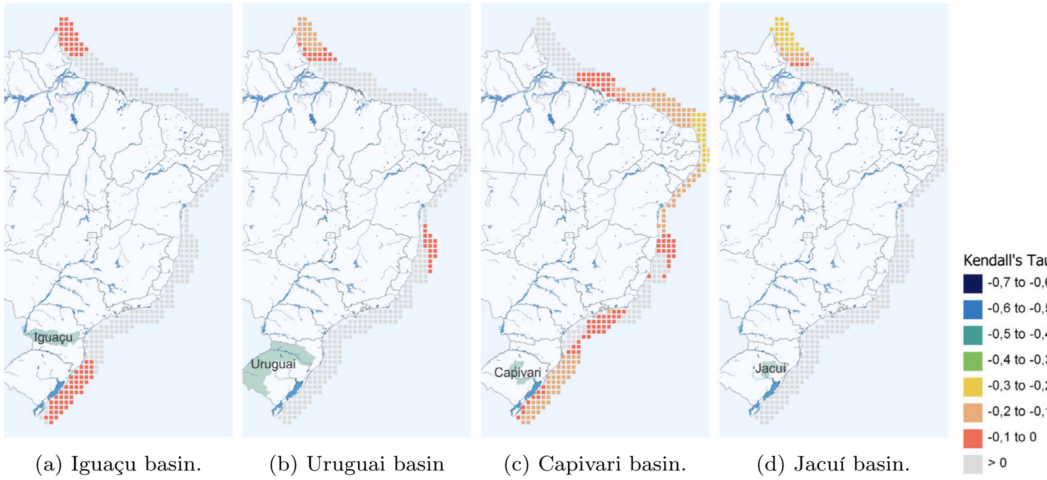

(a) Iguaçu basin. (b) Uruguai basin (c) Capivari basin. (d) Jacuí basin.

Fig. 8. Monthly complementarity between wind power and hydro resources in the Northern and Northeastern basins. Dark blue, blue, and green indicate higher complementarity. Yellow, orange, and red indicate lower complementarity. Gray indicates synergy or no correlation.

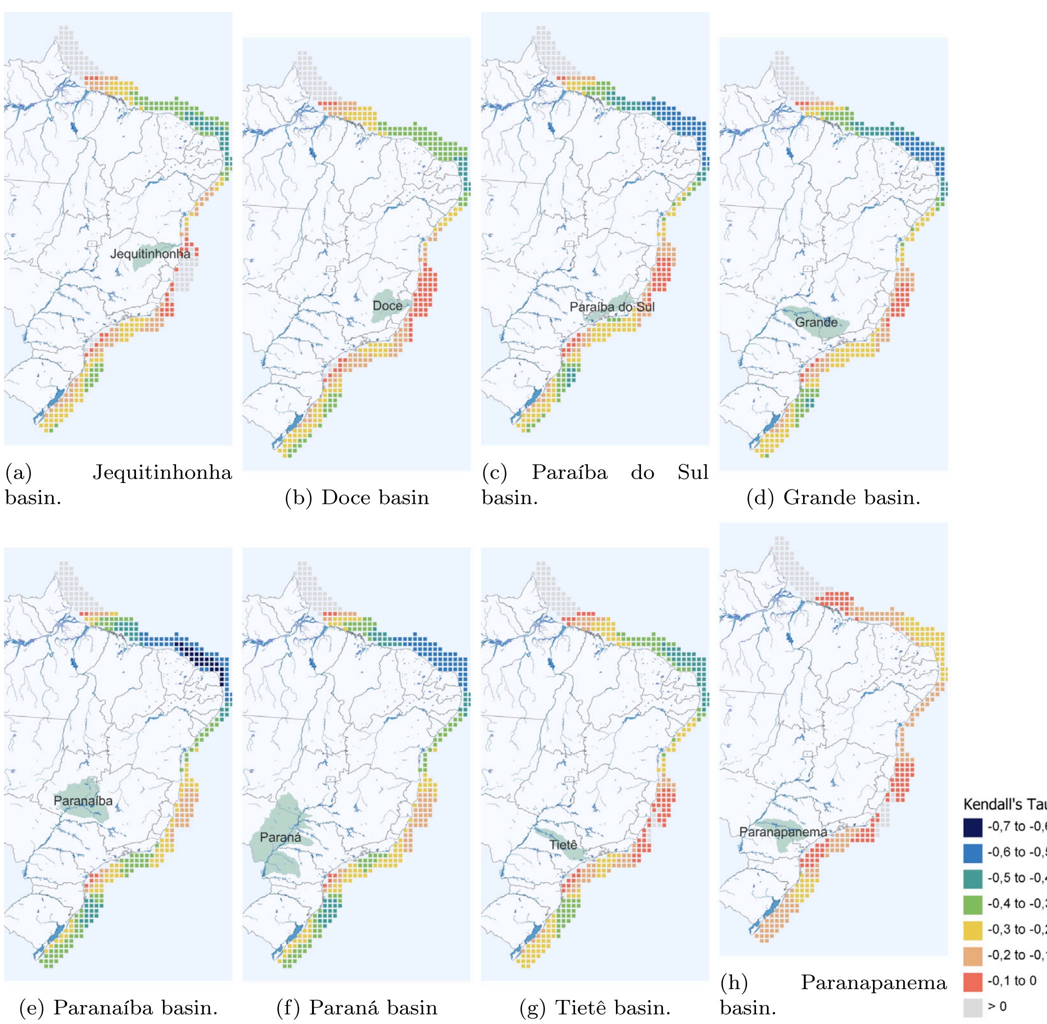

(a) Jequitinhonha basin. (b) Doce basin (c) Paraíba do Sul basin. (d) Grande basin.

(e) Paranaíba basin. (f) Paraná basin (g) Tietê basin. (h) Paranapanema basin.

Fig. 9. Monthly complementarity between wind power and hydro resources in the Northern and Northeastern basins. Dark blue, blue, and green indicate higher complementarity. Yellow, orange, and red indicate lower complementarity. Gray indicates synergy or no correlation.

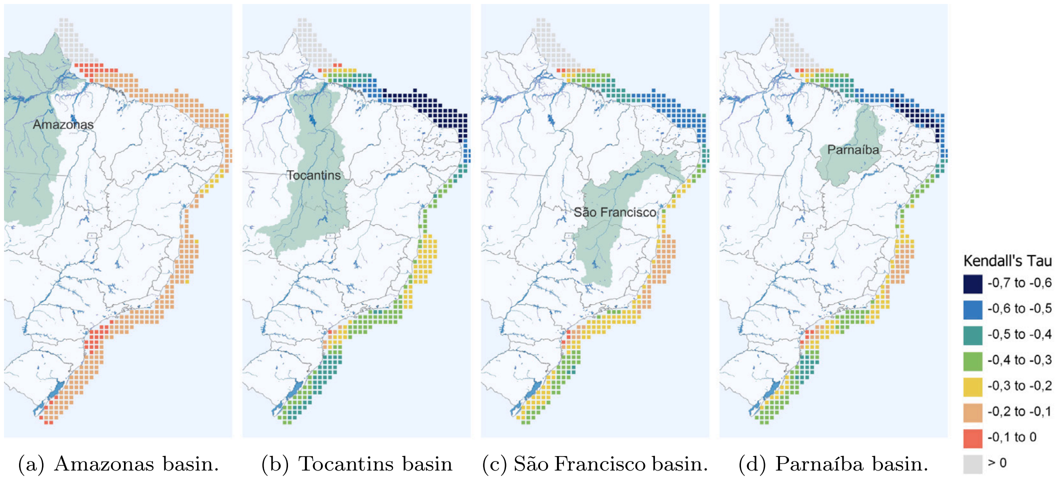

(a) Amazonas basin. (b) Tocantins basin (c) São Francisco basin. (d) Parnaíba basin.

Fig. 10. Monthly complementarity between wind power and hydro resources in the Northern and Northeastern basins. Dark blue, blue and green indicate higher complementarity. Yellow, orange and red indicate lower complementarity. Gray indicates synergy or no correlation.

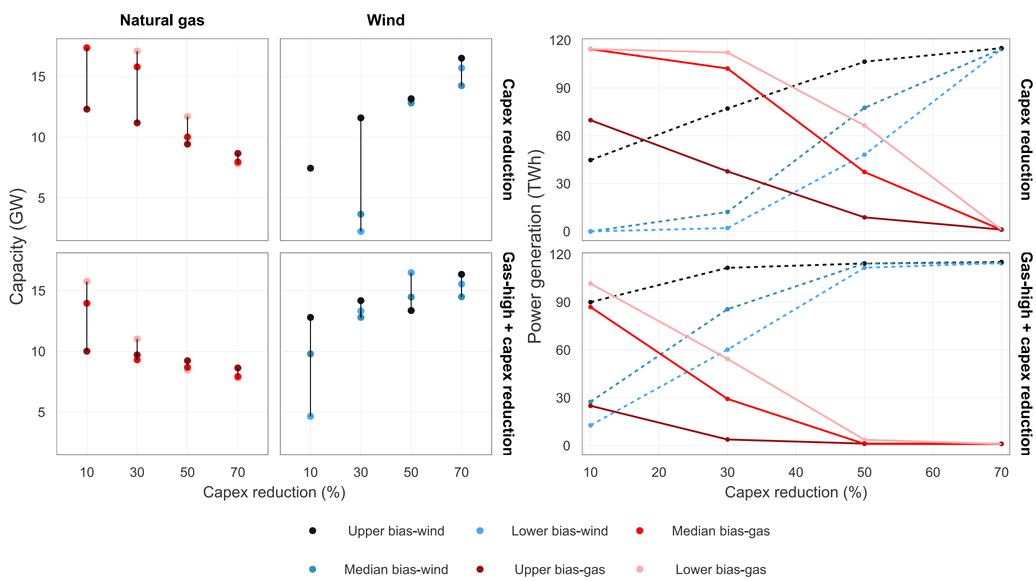

Fig. 11. Capacity and power production of lower, median and upper cases of wind bias correction factor.

Gas-high+OWF-capex-50%. These results imply that although floating structures are more expensive than monopile and jacket, some of the farms located further from shore generate more power than monopile-based farms, reducing their Levelized Costs of Electricity (LCOE) and making them competitive.

Fig. 16 illustrates the LCOE and capacity factor of bottom-fixed and floating technologies. Results reveal LCOE of 121 US$/MWh for monopile no farther than 25 km in Gas-high without reducing the OWF-capex. Bottom-fixed foundations have LCOEs of 96, 82, and 47 US$/MWh with the capex reduction of 30%, 50%, and 70%, respectively. LCOEs of floating structures are 91 and 51 US$/MWh with capex reduced by 50% and 70%. Although these scenarios seem optimistic, they might also be realistic in long-term planning. Wiser et al. [41] suggests cost declines between 37% to 49% in wind farms. Likewise, IRENA [42] estimated a LCOE range between 50 and 90 US$/MWh in 2030 and 30–70 US$/MWh in 2050.

Floating LCOE is higher for locations with a distance of 25 km from the shore than for 75 km. These results differ from the findings of [43], which indicates the distance to shore as the main player in the LCOE increases in Ireland because of the export cable. However, the higher capacity factors compensate for the higher installation costs on the Brazilian coast.

In scenarios with the price increase of natural gas, the LCOEs of wind technologies became higher compared to scenarios where only capex changes.

Findings include the optimal locations for offshore wind farms. The total capacity and the geographical location depend on the year of historical data and the scenario. Fig. 17 shows the results for the average across the weather years and the scenario "Gas-high+OWF-capex 70%", which had the largest capacity of wind farms. Table 3 lists the node ID, geographical location, foundation, and capacity.

The Northeast has a massive installed capacity concentrated in Rio Grande do Norte (RN), Piauí(PI), and Maranhão (MA). Structures are mainly monopile-based. However, in the locations NE_125, NE_127 in Rio Grande do Norte, and NE_139 in Ceará, the model reached the maximal capacity in shallow waters (monopile) and extended to deeper waters, leading to the need for jacket and floating structures. Capacities in Rio de Janeiro (RJ) in the Southeast and Rio Grande do Sul (RS) in the South are also large and requires floating structures.

In June of 2022, the decree 10.946 regulating offshore wind energy exploitation came into force [44]. The decree highlights the rational use of natural resources to enhance energy security. Besides assessing

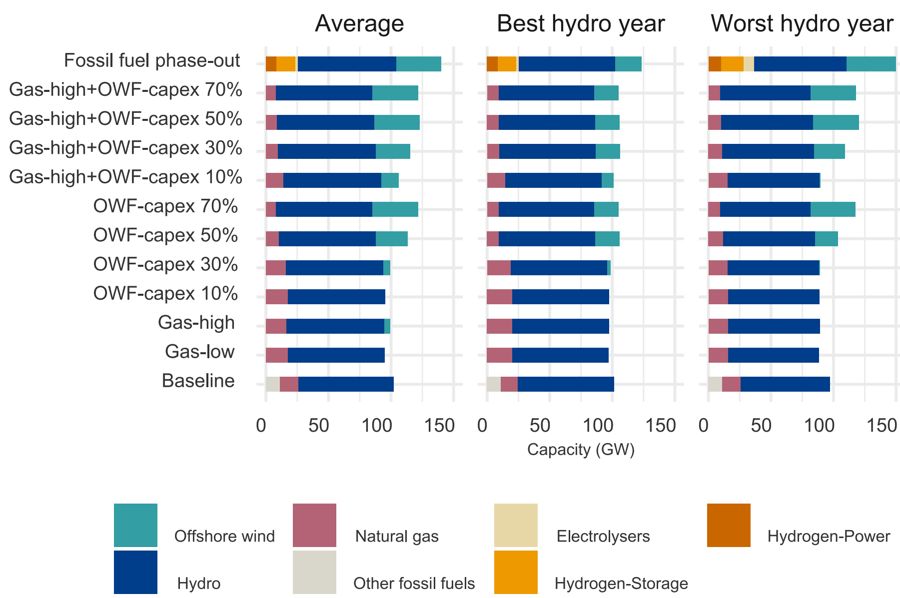

Fig. 12. Capacity of optimal systems in GW.

Fig. 13. Monthly power production: natural gas and offshore wind power. Solid lines mean the median production. The area shaded in red and blue shows the 25th–75th percentile range for the weather years. The vertical region shaded in gray indicates the dry season.

the most cost-attractive offshore regions, this study allows decision-makers to consider synergies with existing fluctuating hydropower to avoid both curtailment and massive amounts of farms in the sea.

3.5. Storage

Existing reservoirs support the integration of offshore wind farms into the system in scenarios with a large share of wind power, but they are not enough in scenarios where fossil fuel is banned. In this case, green hydrogen becomes part of the optimal solution.

Fig. 18 displays the stored hydro resources over a year, on average, for scenarios with OWF-capex reduction and combined with Gas-high. Compared to the baseline scenario, the stored water is reduced in the dry season for scenarios with a larger wind share. That reduction reached 10% in June. Conversely, in these scenarios, stored power increased during the rainy season and reached 6% in December. In the dry season, wind power has a significant impact, implying a reduction of hydro dispatch. With that, reservoirs store water for the rainy season, when wind speeds slow down. The system is thus able to exploit their complementary nature.

Scenarios Gas-high and Gas-low have similar behavior as in scenarios with capex reduced by 10%, where the natural gas share is still significant.

Fig. 19 shows the variation of storage levels in reservoirs when compared to the previous month. For scenarios with more offshore wind farms, the monthly storage variation is nearly 4% lower than the Baseline scenario, except for June and July, when the differences in storage variation are minimal.

Although the storage levels are smaller during the dry season, their monthly variation is less accentuated, leading to more balanced

Table 3
Location details of offshore wind farms resulted from scenario Gas-high+OWF-capex 70%.

Location	State	Lat	Lon	Structure	Capacity (GW)
NE_125	RN	−5.845	−34.921	Monopile, Jacket, Floating	1.66, 2.13, 2.34
NE_127	RN	−5.345	−34.921	Monopile, Jacket, Floating	1.20, 4.00, 5.00
NE_130	RN	−4.845	−35.421	Monopile, Floating	2.77, 1.22
NE_131	RN	−4.845	−35.921	Monopile, Floating	3.42, 2.10
NE_132	RN	−4.845	−36.421	Monopile, Jacket	4.52, 1.94
NE_133	RN	−4.845	−36.921	Monopile	3.40
NE_139	CE	−4.345	−36.921	Monopile, Jacket, Floating	0.62, 1.04, 3.78
NE_162	PI	−2,845	−39,421	Monopile	1.52
NE_168	PI	−2,345	−39,921	Monopile	1.93
NE_169	PI	−2,345	−40,421	Monopile	2.89
NE_170	PI	−2,345	−40,921	Monopile	3.19
NE_171	PI	−2,345	−41,421	Monopile	2.43
NE_172	MA	−2.345	−41.921	Monopile, Jacket	4.56, 7.17
S_231	RS	−29.341	−48.366	Floating	1.80
S_240	RS	−29.841	−48.366	Floating	1.78
S_249	RS	−31.841	−49.421	Floating	2.00
S_251	RS	−30.841	−49.886	Floating	1.37
SE_301	RJ	−23.841	−40.866	Floating	3.12
SE_306	RJ	−23.841	−41.366	Floating	7.2

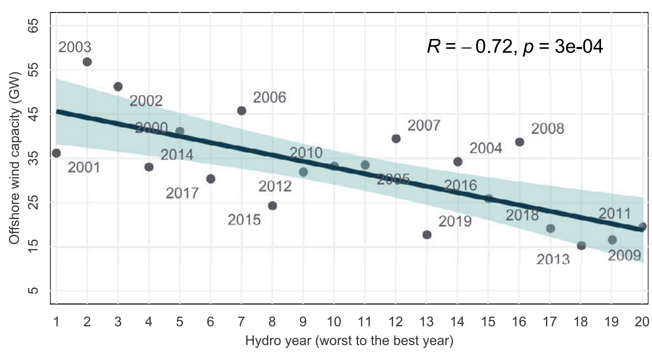

Fig. 14. Sensitivity analysis of wind capacity in different weather years.

systems. The increase in wind power leads to two main implications for reservoirs. First, the risk of having empty reservoirs in the rainy season is reduced. Avoiding critical water storage levels contributes to better management of hydro resources, including urban water supply, irrigation, and protection of aquatic fauna. Further, the energy system might also benefit. When reservoirs are full, evaporation rates are increased, which reduces air temperature in the regional climate system [45]. In turn, with a more humid and cooler atmosphere, the air becomes denser, and precipitation chances increase. Therefore, such system might be able to produce even more electricity from hydropower plants compared to the current one.

3.6. Emissions

Fig. 20 shows the indirect and direct emissions from offshore wind farms, CCGT plants burning natural gas, and coal and oil-fired power stations and indicates their variability over different weather years.

The baseline scenario results in average emissions of 56 Mton $CO_{2_{eq}}$/year. This result is in line with the 50.6 Mton $CO_{2_{eq}}$ emissions in 2019 (excluding isolated systems) reported by EPE [46]. The findings suggest a significant reduction of emissions in scenarios with capex reduced by 70% and Gas-high+OWF-capex 50%, which have the largest wind capacity. In these scenarios, emissions are at an average of 1.6 Mton $CO_{2_{eq}}$, suggesting avoidance of 54.4 Mton $CO_{2_{eq}}$/year from the power sector, or elimination of nearly 97% of power sector emissions. Less ambitious scenarios, such as "Gas-high+OWF-capex-10%", have, on average, emissions around 13 Mton $CO_{2_{eq}}$ less than the Baseline scenario. However, in scenarios with capex reduced by 10% and 30%, or with a high gas price, the contribution to decreasing $CO_{2_{eq}}$ is less significant.

Systems with a considerable share of natural gas had higher standard deviations over the years. Thus, these configurations are more vulnerable to having larger and more variable annual $CO_{2_{eq}}$ emissions since the thermal dispatch occurs in periods of lower hydro availability. Once the system integrates more wind farms, gas power dispatch plays a smaller role over the year, as an increasingly higher fraction of hydro variability is balanced by wind power.

With the privatization of Eletrobras (a company responsible for one-third of Brazil's total installed capacity) in June of 2022, the power system will have an extra 6 GW of CCGT by 2028 (for a total of 32 GW of fossil-fired power stations) and a mandatory contracting of 70% of inflexible natural gas. That would increase GHG emissions from the power sector by 24.6% (or 13 Mton $CO_{2_{eq}}$/year, considering the year 2019) [47]. Results suggest that no extra CCGT would be necessary for scenarios with a high share of offshore wind power. Instead, wind farms could be promoted and subsidized to meet the National Program of Green Growth (PNCV[1]) goals, which aim to reduce GHG emissions, provide incentives for mitigating and adapting to climate change and establish a green economy.

4. Conclusion

This work investigates three main issues for offshore wind in a power system highly dependent on variable renewable energy using Brazil as a case study. First, the bias correction analysis of MERRA-2-based wind power was carried out and provided accurate data to investigate the role of offshore wind farms. Second, this study explored the complementarity between hydro and offshore wind resources quantitatively. Finally, the third step consisted in integrating offshore wind farms into the existing power system through an optimization model, which could be reproducible for other countries with the appropriate inputs.

MERRA-2 based wind power simulation presented significant bias. In most cases, MERRA-2 overpredicts the wind power, but underpredicts in Rio de Janeiro (RJ), Pernambuco (PE), and some wind parks in Piauí(PI). Without bias correction, the total potential of offshore wind energy sums up to 2366 TWh/yr for locations with a capacity factor higher than 45%. It decreases by 8%, 25%, and 44% for the upper, median, and lower bias cases, respectively.

The findings suggested a high wind-hydropower complementarity, particularly between wind regimes in the Northeast and basins in the Southeast-Midwest and Northeast. Southern basins and the Amazonas basin have low or no complementarity with wind at the coast.

[1] Programa Nacional de Crescimento Verde, created in October 2021.

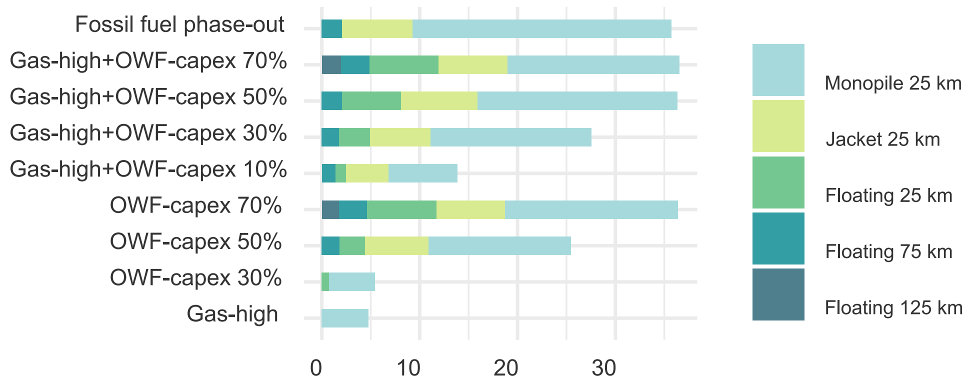

Fig. 15. Offshore wind capacity in GW.

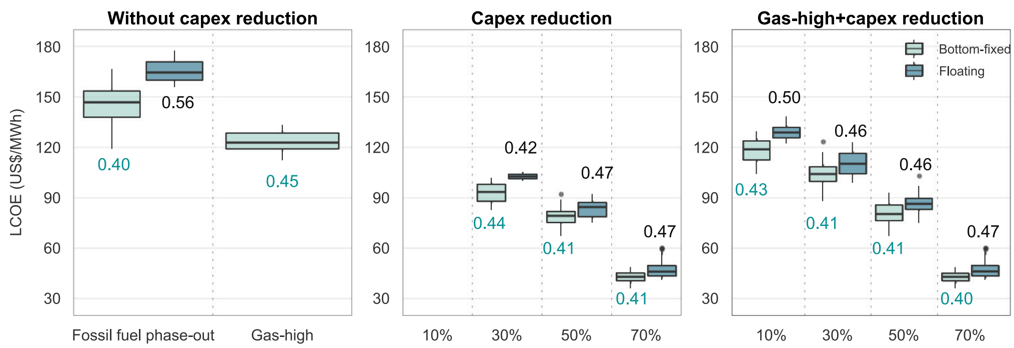

Fig. 16. LCOE of bottom-fixed and floating structures. The numbers above or below the boxes indicate the average capacity factor.

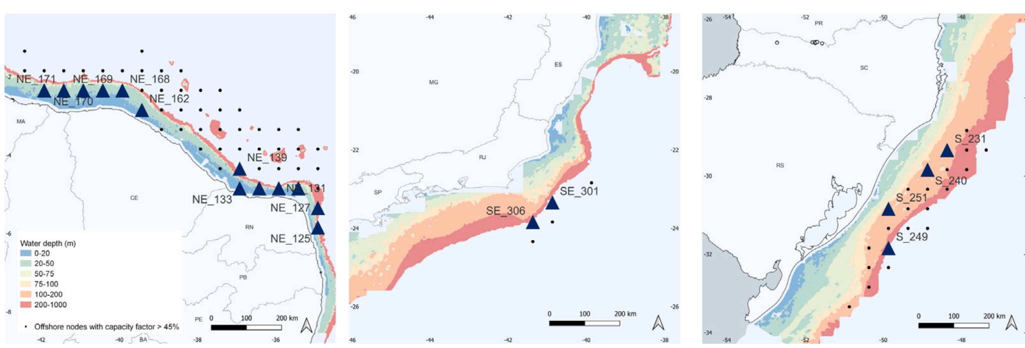

(a) Northeast. (b) Southeast. (c) South.

Fig. 17. Locations of offshore wind farms in the scenario Gas-high+OWF-capex 70%.

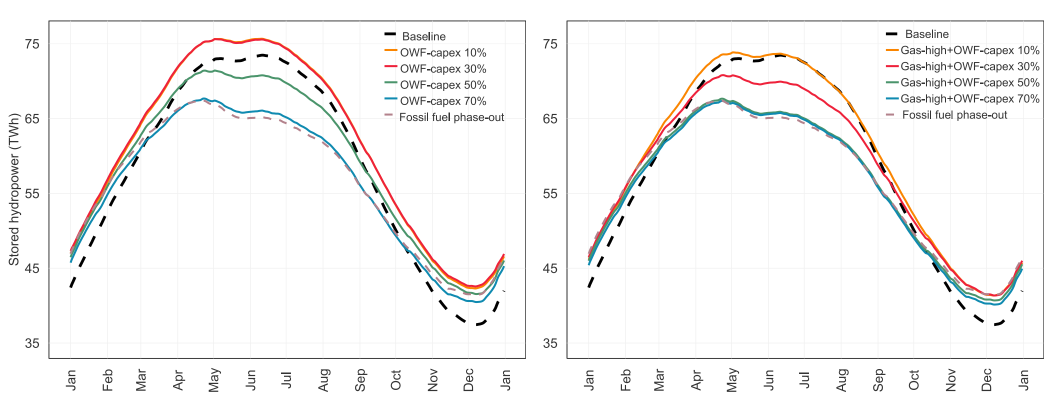

(a) OWF-capex reduction scenarios. (b) Gas-high+OWF-capex reduction scenarios.

Fig. 18. Daily stored hydropower in TWh.

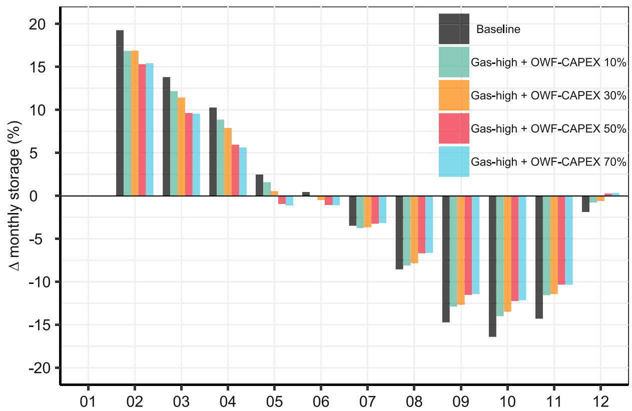

Fig. 19. Monthly variation of storage levels in reservoirs.

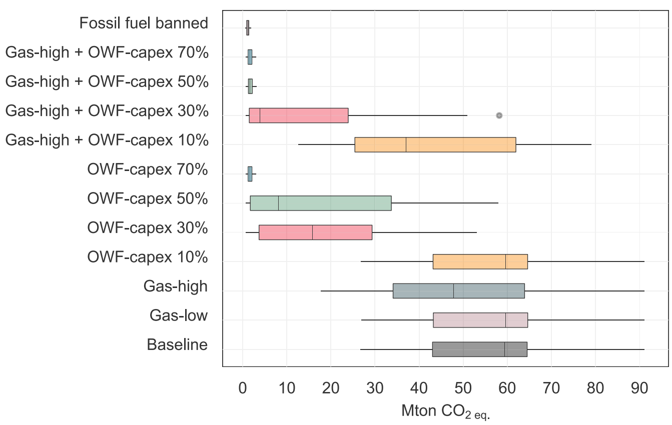

Fig. 20. Range of emissions in different weather years.

The LCOEs of monopile-based wind farms are on average 121 US$/MWh without capex reduction. LCOEs are 87 and 49 US$/MWh in scenarios with capex reduced by 50% and 70%, respectively. Results suggest a potential cost competitiveness for offshore wind energy in Brazil and a purely cost-related reason to phase out natural gas-fired generation.

Storage technologies are essential to smooth the power fluctuation of renewable energy and maximize their share in the system. Results showed that it is possible to have a highly renewable power system with no need for new reservoirs or extra storage technologies. This is a unique feature of the Brazilian system with its very high reliance on hydropower. Yet it was observed that current reservoir dynamics change with the integration of wind technologies into the system. Current operation prioritizes storage during the rainy periods to use the power later in the dry season when hydro resources are scarcer. With the increase in offshore wind share, reservoirs still store more water during the dry period. However, the storage is reduced in the dry season compared to the baseline scenario. Still, it increases in the rainy season since offshore wind has a bigger role during the dry periods. Such a system might be able to produce even more electricity from hydropower plants compared to the current one due to its less accentuated monthly variation of storage levels and, consequently, higher chances of precipitation.

Emissions in the baseline scenarios sum to 56 Mton $CO_{2_{eq}}$/year on an average of 20 years. Offshore wind farms contribute to a reduction of 52.8 Mton $CO_{2_{eq}}$/year in scenarios with the largest share of wind power. On the other hand, in scenarios where natural gas is still relevant, the emission decline is less significant. Also, in systems with natural gas and hydro resources, the emissions are highly dependent on the weather year. In contrast, the integration of offshore wind energy notably reduces the standard deviation over the years. Under climate change scenarios, the emission variability might be higher due to the uncertainty of hydro availability. That might also be an issue in elaborating plans and accomplishing commitments to reduce GHG. Thus, offshore wind energy minimizes uncertainties about emissions from the power sector.

Future studies could include other renewable technologies, non-electric energy-using sectors (especially industry and transportation), and a detailed consideration of the transmission system to fully assess sustainable options for the Brazilian energy system. Although this work included hydrogen, it did not appear as a cost-competitive resource for the power sector in the scenarios where fossil fuels are allowed. Further investigation is necessary to understand the benefits of green hydrogen when considering the other energy-using sectors and the possibility of exports to other countries. Finally, improvements to the wind potential assessment are possible. The distance to shore instead of the distance to harbors was used for cost calculations. Depending on the wind farm location and the lack of existing infrastructure, their installation costs could be higher than the estimated cost.

Nevertheless, the results provide novel insight into the potential for Brazil to eliminate much of its power-sector-related GHG emissions. Results suggest that no extra CCGT would be necessary for scenarios with a high share of offshore wind power. Also, the findings may guide the integration of offshore wind farms into the power system and help design the priority regions for offshore wind development in line with Brazil's policy goals.

CRediT authorship contribution statement

Paula Conde Santos Borba: Conceptualization, Methods, Software, Writing – original draft, Visualization. **Wilson C. Sousa Júnior:** Methods, Writing – review & editing, Supervision. **Milad Shadman:** Methods, Writing – review & editing. **Stefan Pfenninger:** Conceptualization, Methods, Writing – review & editing, Supervision.

Declaration of competing interest

The authors declare that they have no known competing financial interests or personal relationships that could have appeared to influence the work reported in this paper.

Acknowledgment

This study was financed in part by the Coordenação de Aperfeiçoamento de Pessoal de Nível Superior – Brasil (CAPES) – Finance Code 001.

Appendix A. Supplementary data

Supplementary material related to this article can be found online at https://doi.org/10.1016/j.enconman.2022.116616.

References

[1] IEA. Data and statistics - Electricity generation by source. 2019, https://www.iea.org/data-and-statistics/data-browser?country=WORLD&fuel=Electricity%20and%20heat&indicator=WasteGenBySourcer, [Online; accessed 24-Mar-2022].

[2] Siala K, Chowdhury AK, Dang T, Galelli S. Solar energy and regional coordination as a feasible alternative to large hydropower in Southeast Asia. Nature Commun 2021;12:4159. http://dx.doi.org/10.1038/s41467-021-24437-6.

[3] Sun F, Wang T, Wang H. Mapping global GDP exposure to drought. In: Atlas of global change risk of population and economic systems. Springer; 2022, p. 123–30.

[4] IPCC. Climate change 2021: The physical science basis. Contribution of working group I to the sixth assessment report of the intergovernmental panel on climate change. Cambridge University Press; 2021.

[5] Getirana A, Libonati R, Cataldi M. Brazil is in water crisis — it needs a drought plan. Nature 2021;600:218–20. http://dx.doi.org/10.1038/d41586-021-03625-w.

[6] Langenbrunner B. Water, water not everywhere. Nature Clim Change 2021;11:650. http://dx.doi.org/10.1038/s41558-021-01111-9.

[7] Aneel. Capacidade instalada. 2022, https://www.gov.br/aneel/pt-br/assuntos/noticia/2022/expansao-na-matriz-eletrica-foi-de-200-mw-em-abril-com-acrescimos-em-cinco-estados, [Online; accessed 16-June-2022].

[8] ONS. Data: Carga e geração. 2019, http://www.ons.org.br/paginas/energia-agora/carga-e-geracao, [Online; accessed 24-Mar-2022].

[9] EPE. Plano nacional de energia 2050. 2020, URL https://www.epe.gov.br/sites-pt/publicacoes-dados-abertos/publicacoes/PublicacoesArquivos/publicacao-227/topico-563/Relatorio%20Final%20do%20PNE%202050.pdf.

[10] Díaz H, Guedes Soares C. Review of the current status, technology and future trends of offshore wind farms. Ocean Eng 2020;209:107381. http://dx.doi.org/10.1016/j.oceaneng.2020.107381.

[11] Voormolen J, Junginger H, van Sark W. Unravelling historical cost developments of offshore wind energy in Europe. Energy Policy 2016;88:435–44. http://dx.doi.org/10.1016/j.enpol.2015.10.047.

[12] Virtanen E, Lappalainen J, Nurmi M, Viitasalo M, Tikanmäki M, Heinonen J, Atlaskin E, Kallasvuo M, Tikkanen H, Moilanen A. Balancing profitability of energy production, societal impacts and biodiversity in offshore wind farm design. Renew Sustain Energy Rev 2022;158:112087. http://dx.doi.org/10.1016/j.rser.2022.112087.

[13] Bosch J, Staffell I, Hawkes AD. Temporally explicit and spatially resolved global offshore wind energy potentials. Energy 2018;163:766–81. http://dx.doi.org/10.1016/j.energy.2018.08.153.

[14] Vinhoza A, Schaeffer R. Brazil's offshore wind energy potential assessment based on a spatial multi-criteria decision analysis. Renew Sustain Energy Rev 2021;146:111185. http://dx.doi.org/10.1016/j.rser.2021.111185.

[15] EPE. Roadmap eólica offshore Brasil. 2020.

[16] Silva AR, Pimenta FM, Assireu AT, Spyrides MHC. Complementarity of Brazil's hydro and offshore wind power. Renew Sustain Energy Rev 2016;56:413–27.

[17] Gonzalez-Salazar M, Poganietz WR. Evaluating the complementarity of solar, wind and hydropower to mitigate the impact of El Niño Southern Oscillation in Latin America. Renew Energy 2021;174:453–67. http://dx.doi.org/10.1016/j.renene.2021.04.048.

[18] dos Reis MML, Mazetto BM, da Silva ECM. Economic analysis for implantation of an offshore wind farm in the Brazilian coast. Sustain Energy Technol Assess 2021;43:100955.

[19] Staffell I, Pfenninger S. Using bias-corrected reanalysis to simulate current and future wind power output. Energy 2016;114:1224–39. http://dx.doi.org/10.1016/j.energy.2016.08.068.

[20] Gruber K, Klöckl C, Regner P, Baumgartner J, Schmidt J. Assessing the global wind atlas and local measurements for bias correction of wind power generation simulated from MERRA-2 in Brazil. Energy 2019;189:116212. http://dx.doi.org/10.1016/j.energy.2019.116212.

[21] de Assis Tavares LF, Shadman M, de Freitas Assad LP, Silva C, Landau L, Estefen SF. Assessment of the offshore wind technical potential for the Brazilian Southeast and South regions. Energy 2020;196:117097. http://dx.doi.org/10.1016/j.energy.2020.117097.

[22] Latinopoulos D, Kechagia K. A GIS-based multi-criteria evaluation for wind farm site selection. A regional scale application in Greece. Renew Energy 2015;78:550–60. http://dx.doi.org/10.1016/j.renene.2015.01.041.

[23] CPRM. Batimetria. 2019, http://www.cprm.gov.br/publique/Geologia/Geologia-Marinha/Projeto-Batimetria-3224.html, [Online; accessed 25-April-2020].

[24] Marques AT, Santos CD, Hanssen F, Muñoz A-R, Onrubia A, Wikelski M, Moreira F, Palmeirim JM, Silva JP. Wind turbines cause functional habitat loss for migratory soaring birds. J Anim Ecol 2020;89(1):93–103. http://dx.doi.org/10.1111/1365-2656.12961.

[25] Gelaro R, McCarty W, Suárez M, Todling R, Molod A, Takacs L, Randles C, Darmenov A, Bosilovich M, Reichle R, Wargan K, Coy L, Cullather R, Draper C, Akella S, Buchard V, Conaty A, Da Silva A, Gu W, Zhao B. The modern-era retrospective analysis for research and applications, version 2 (MERRA-2). J Clim 2017;30. http://dx.doi.org/10.1175/JCLI-D-16-0758.1.

[26] Pookpunt S, Ongsakul W. Design of optimal wind farm configuration using a binary particle swarm optimization at Huasai district, Southern Thailand. Energy Convers Manage 2016;108:160–80. http://dx.doi.org/10.1016/j.enconman.2015.11.002.

[27] CPTEC. Estações. 2021, http://clima1.cptec.inpe.br/estacoes/, [Online; accessed 20-May-2021].

[28] ONS. Construção da curva referencial de armazenamento- CREF -para o ano de 2021. 2021, https://www.gov.br/mme/pt-br/assuntos/conselhos-e-comites/cmse/atas/2021/anexo-4_nt-ons-dpl-0021-2021-metodologia-curva-referencial-2021.pdf, [Online; accessed 24-Mar-2022].

[29] Jurasz J, Canales F, Kies A, Guezgouz M, Beluco A. A review on the complementarity of renewable energy sources: Concept, metrics, application and future research directions. Sol Energy 2020;195:703–24. http://dx.doi.org/10.1016/j.solener.2019.11.087.

[30] Ren G, Wan J, Liu J, Yu D. Spatial and temporal assessments of complementarity for renewable energy resources in China. Energy 2019;177. http://dx.doi.org/10.1016/j.energy.2019.04.023.

[31] Pfenninger S, Pickering B. Calliope: a multi-scale energy systems modelling framework. J Open Source Softw 2018;3(29):825. http://dx.doi.org/10.21105/joss.00825.

[32] Maness M, Maples B, Smith A. NREL offshore balance-of-system model. 2017, http://dx.doi.org/10.2172/1339522, URL https://www.osti.gov/biblio/1339522.

[33] Armijo J, Philibert C. Flexible production of green hydrogen and ammonia from variable solar and wind energy: Case study of Chile and Argentina. Int J Hydrogen Energy 2020;45(3):1541–58. http://dx.doi.org/10.1016/j.ijhydene.2019.11.028.

[34] NREL. 2021 annual technology baseline (ATB) cost and performance data for electricity generation technologies. 2019, https://data.openei.org/submissions/4129, [Online; accessed 24-Mar-2022].

[35] IPCC. Technology-specific cost and performance parameters. In: Climate change 2014: Mitigation of climate change: Working group III contribution to the IPCC fifth assessment report. Cambridge University Press; 2015, p. 1329–56. http://dx.doi.org/10.1017/CBO9781107415416.025.

[36] ONS. Curva de carga horária. 2020, http://www.ons.org.br/Paginas/resultados-da-operacao/historico-da-operacao/curva_carga_horaria.aspx, [Online; accessed 08-June-2020].

[37] Gruber K, Regner P, Wehrle S, Zeyringer M, Schmidt J. Towards global validation of wind power simulations: A multi-country assessment of wind power simulation from MERRA-2 and ERA-5 reanalyses bias-corrected with the global wind atlas. Energy 2022;238:121520. http://dx.doi.org/10.1016/j.energy.2021.121520.

[38] Schaeffer R, Szklo A, de Lucena AFP, Soria R, Chavez-Rodriguez M. The vulnerable amazon: The impact of climate change on the untapped potential of hydropower systems. IEEE Power Energy Mag 2013;11(3):22–31. http://dx.doi.org/10.1109/MPE.2013.2245584.

[39] Molina Carpio J, Espinoza J, Vauchel P, Ronchail J, Caloir B, Guyot J-L, Noriega L. Hydroclimatology of the Upper Madeira River basin: spatio-temporal variability and trends. Hydrol Sci J 2017;62:911–27. http://dx.doi.org/10.1080/02626667.2016.1267861.

[40] Espinoza J, Sörensson A, Ronchail J, Molina Carpio J, Segura H, Gutierrez-Cori O, Ruscica RC, Condom T, Wongchuig S. Regional hydro-climatic changes in the Southern Amazon Basin (Upper Madeira Basin) during the 1982–2017 period. J Hydrol: Reg Stud 2019;26. http://dx.doi.org/10.1016/j.ejrh.2019.100637.

[41] Wiser R, Rand J, Seel J, Beiter P, Baker E, Lantz E, Gilman P. Expert elicitation survey predicts 37 costs by 2050. Nat Energy 2021;2021. http://dx.doi.org/10.1038/s41560-021-00810-z.

[42] IRENA. Future of wind. Deployment, investment, technology, grid integration and socio-economic aspects (A Global Energy Transformation paper). Abu Dhab: Renewable Energy Agency; 2019.

[43] Martinez A, Iglesias G. Site selection of floating offshore wind through the levelised cost of energy: A case study in Ireland. Energy Convers Manage 2022;266:115802. http://dx.doi.org/10.1016/j.enconman.2022.115802, URL https://www.sciencedirect.com/science/article/pii/S0196890422005982.

[44] Brazil. Decreto n° 10.946, DE 25 DE Janeiro DE 2022. 2022, http://www.planalto.gov.br/ccivil_03/_Ato2019-2022/2022/Decreto/D10946.htm, [Online; accessed 15-Jun-2022].

[45] Hunt JD, Nascimento A, ten Caten CS, Tomé FMC, Schneider PS, Thomazoni ALR, de Castro NJ, Brandão R, de Freitas MAV, Martini JSC, Ramos DS, Senne R. Energy crisis in Brazil: Impact of hydropower reservoir level on the river flow. Energy 2022;239:121927. http://dx.doi.org/10.1016/j.energy.2021.121927.

[46] Empresa de Pesquisa Energética. Anuário estatístico de energia elétrica. EPE; 2020, URL https://www.epe.gov.br/pt/publicacoes-dados-abertos/publicacoes/anuario-estatistico-de-energia-eletrica.

[47] IEMA. Questionamentos à inserção de termelétricas a gás natural na Medida Provisória 1.031/2021. IEMA; 2021.